G-Scidar measurements of the Optical Turbulence with standard and high vertical resolution at Mt.Graham

Jeff Stoesz[a], Elena Masciadri[a], Susanna Hagelin[a,b], Franck Lascaux[a] and Sebastian Egner[c]

[a]Osservatorio Astrofisico di Arcetri, Largo Enrico Fermi 5, 50125 Firenze, Italy;
[b]Uppsala Universitet, Department of Earth Sciences, Villavägen 16, S-752 36 Uppsala, Sweden;
[c]Max-Planck-Institut für Astronomie, Koenigstuhl 17, 69117 Heidelberg, Germany

ABSTRACT

Since November 2004 we measured the optical turbulence (C_N^2 profiles) with a Generalized Scidar (GS) placed at the focus of the Vatican Advanced Technology Telescope at Mt.Graham, Arizona. The present statistic consists in measurements related to 43 nights covering different periods of the solar year. In this paper we calculate the statistics of the astroclimatic parameters (C_N^2 , seeing ε , isoplanatic angle θ_0, wavefront coherence time τ_0) and we compare these values with those measured above other top level astronomic sites. All profiles are reduced into a form suitable to be used as inputs for adaptive optics point spread function simulations for the conceptual design of the Laser Guide Star Facility supported by a GLAO system of the Large Binocular Telescope. With GS measurements done observing wide binaries (30-35 arcsec), the turbulence in the first kilometer above the ground is characterized with the vertical resolution (200-250 m) required for the optimization of a 4 arcmin field of view AO system. It is the first time that are published measurements of the optical turbulence vertical distribution above a mid-latitude site with such a high vertical resolution and such a high statistical reliability. On 8 of those nights, employing cross-correlation scintillation maps of wide binaries and the method described in Ref.[1] we characterize the distribution of the optical turbulence in the first kilometer at the extremely high vertical resolution of 20-30 meters.

Keywords: turbulence, site testing, atmospheric effects, image processing

1. INTRODUCTION

The optical turbulence measurement campaigns at Mt. Graham, with the first 16 nights thoroughly analysed and published,[2] collected so far measurements on 43 different nights. Measurements of the C_N^2 profiles have been obtained with a Generalized Scidar (GS) placed at the focus of the 2-meter class Vatican Advanced Technology Telescope (VATT) on the Mt.Graham summit, around 250 m far away from the Large Binocular Telescope (LBT). This long-term site testing campaign aims:
(1) To collect an as rich as possible statistical sample of optical turbulence vertical distribution (C_N^2 profiles) to be compared with simulations obtained with mesoscale atmospheric models.[3] This is a key milestone for the ForOT project* whose final goal is to predict the optical turbulence above astronomical sites.[4]
(2) To provide a characterization of all the most important integrated astroclimatic parameters above the site of the Large Binocular Telescope (LBT).
(3) To provide an as rich as possible statistical sample of optical turbulence vertical distribution at high resolution in the first hundreds of meters. This is a key element for the feasibility study of the LGS/GLAO system conceived for the LBT (Rabien et al. 2008, this Conference).

We use the high vertical resolution (HVR) technique[1] to reconstruct the vertical distribution of the turbulence in the first hundreds of meters with a vertical resolution of 20-30 meters. This new method is based on the observation of wide binaries ($\sim$ 30-35 arcsec) and the simultaneous calculation of the auto and cross-correlation of the scintillations maps. The vertical resolution is not defined by the intrinsic GS resolution but by the accuracy

Further author information: (Send correspondence to J.S. or E.M.)
E-mail: stoesz@arcetri.astro.it, masciadri@arcetri.astro.it, Telephone: +39 055 2752 203
*$http://forot.arcetri.astro.it$

Ground-based and Airborne Telescopes II, edited by Larry M. Stepp, Roberto Gilmozzi,
Proc. of SPIE Vol. 7012, 70121W, (2008) · 0277-786X/08/$18 · doi: 10.1117/12.789653

with which we can locate the lateral peaks of the cross-correlation triplets. It has been shown[1] that this is of the order of 20-30 m.

As shown in Fig.4,[1] the LBT is located at the summit of Mt. Graham and built on a very high pier, which puts its primary mirrors about 30 meters above the ground. Unlike the VATT, whose dome is at the level of the treetops, the LBT is located well above the treetops (20 m) and in the past it has been shown that this distance is enough large to mitigate potential turbulence effects due to the interaction of the atmospheric flow with the treetops. The HVR technique permits, among others things, to quantify the contribution of the optical turbulence developed below the primary mirror of the LBT.

In the next subsection we briefly describe our Generalized Scidar system and give references to Scidar theory. In Sec. 2, we describe the automatic observing campaign's data reduction pipeline to calculate the strength (C_N^2) and height (h), as well as the completeness for the wind measurements. In Sec. 3 we present statistics of the C_N^2 profiles and all the main integrated astroclimatic parameters. The optical turbulence vertical distribution related to our sample (43 nights) is compared to that obtained with vertical profilers (GS and the MASS[†]) above other sites. We highlight that the statistical samples related to these sites are not equally dense (from a few nights up to several tens of nights) therefore the statistic reliability of this result needs to be taken and used with some precaution. In Sec.4 we provide an analysis of the optical turbulence vertical distribution in the first few hundreds of meters. We finally summarize the conclusions in Sec.5.

1.1 The Scidar system

The Scidar instrument was built to fit the 1.75 meter telescope of the VATT observatory for LBT site testing.[6] VATT is located near the summit of Mt. Graham, Arizona, and about 250 meters west of the LBT. The video rate CCD detector has a 256x256 array and is coupled to an image intensifier. The intensifier is gated to achieve a 1 ms exposure per elemental frame, at a frame rate of 100 Hz. The wavelength is $0.5\mu m$. The conjugation plane of the system is adjustable by moving the detector-intensifier stage. It is fixed at the beginning of an observing run at a distance of 3.5-4.2 km below the ground. The system computes auto-correlation and cross-correlation simultaneously in real-time and stores them in *fits format* image files. The reader can refer to [2] as well as the precedent papers [7–9] for more details on the Scidar concept.

The VATT has an active thermal control system for its primary mirror as well as a strong ventilation system. The system turned on at or before dusk and, once equilibrium is reached, keeps the primary mirror within one degree Celsius of the ambient temperature. Just a few cases in which $\Delta T \geq 1$ C$^\circ$ has been observed so far. The ventilation system is able to maintain a good flow of air into the dome through the telescope aperture. As part of this system there are numerous thermocouple sensors in the dome. During the more recent observing runs we have recorded 1) mean temperature from two sensors in the air near the telescope's line of sight, but inside the dome, 2) the mean temperature of two sensors in thermal contact with the metal structure that supports the telescope's secondary mirror, and 3) the temperature of the primary mirror itself.

2. DATA REDUCTION

Table 1 shows the classification of the 35,516 measurements collected so far since November 2004. The measurements obtained with the GS in the so called standard configuration (A. in Table 1) are those which sample the whole 20 km above Mt. Graham with the typical vertical resolution given by Eq.2 - Ref.[1] ($\sim$ 1 km near the ground). The standard GS measurements count now 16,657 profiles, or 163 hours, which increases a factor 4 from the 41.7 hours in the original 16 nights before to 2007.

With our optical set-up in the standard GS configuration, the binary stars need a separation θ within (3-8) arcsec, $\Delta m \leq 1.5$ mag and m_1, $m_2 \leq$ 5-6 mag (Table 2). Using wide binaries ($\theta \sim 30$ arcsec) and the auto-correlation one can increase the vertical resolution of a factor ~ 4 with respect to the standard GS. We will call hereafter this intermediate vertical resolution with the 'WB' label. Using the wide-binaries and the 'HVR method'[1] i.e. the auto and the cross-correlations maps, we can increase the vertical resolution of a factor ~ 20 and reach a $\Delta h =$ 20-30 m.

[†]Multi-Aperture Scintillation Sensor

Table 1. Classification of the Scidar campaign measurements. **GS standard:** the vertical resolution scales with h as Eq.2 - Ref.[1]. It is typically of the order of 1000 m near the ground. **GS - WB:** the vertical resolution of the order of 250 m. Measurements are related to the first kilometer above the ground. The C_N^2 profiles are retrieved from the auto-correlation of scintillation maps of wide-binaries ($\sim$ 30 arcsec). **GS - HVR:** the vertical resolution is of the order of 20-30 m. The method is described in Ref.[1]

Selected Samples:	Nights	Number of meas.	Number of hours
A. GS standard	43	16,657	163
B. GS - WB	23	5,412	13.5
C. GS - HVR	8	1,894	3.3
Observing Runs:			
2005 Apr 27	1	550	3.8
2005 May 19-24	6	2,988	17.9
2005 Dec 6-15	5	3,778	31.7
2007 May 27 - June 3	8	5,296	32.2
2007 Oct 16-28	13	10,998	85.8
2008 Feb 23 - Mar 3	10	8,140	73.8

Table 2. Binary Stars Parameters

Binary Star Name	RA J2000	Dec J2000	m_1 (V mag)	m_2 (V mag)	Separation (arcsec)
γ Ari	01 54	+19 17	4.5	4.6	7.6
Castor	07 35	+31 53	1.9	3.0	4.4
γ Leo	10 20	+19 50	2.4	3.6	4.7
π Boo	14 41	+16 25	4.9	5.8	5.5
δ Ser	15 34	+10 32	4.2	5.2	4.1
95 Her	18 02	+21 36	4.9	5.2	6.5
β Cyg	19 31	+27 58	3.2	4.7	35.3

2.1 C_N^2 profiles

To retrieve a C_N^2 profile one has to calculate the average of the auto-correlation of the scintillation maps, normalized by the auto-correlation of the average of the scintillation maps obtained on the CCD.

From the 2-D auto-correlation array we calculate the difference of sections (1-D arrays) parallel and perpendicular to the star separation to eliminate the contribution of the central peak in which is concentrated the correlated noise of the camera. Note that our software works in polar coordinates instead of the more common system (x, y). The background noise is estimated from a slit extracted in a region of the auto-correlation in which the signal is not present and then subtracted from the 1-D array containing the signal information.

The 1-D cut of the 2-D auto-correlation is then used to compute the C_n^2 profile by inverting equation 1 of [2] using a conjugate gradient method. Due to the fact that the scintillation effect is accumulated over a distance in the neighbourhood of h_i, we get the turbulence integral J_i or the average-discretized C_n^2 , written

$$C_{ni}^2(h_i) = \frac{J_i(h_i)}{\Delta h}. \quad (1)$$

The Δh is the regular spacing between auto-correlation pixels, $h_{i+1} - h_i$.

The stellar parameters are extracted from the WDS catalogue[10] and are reported in Table 2. The only significant update with respect to the WDS catalogue used by [1,2] is a 5% difference in the separation of Castor.

2.2 Wind data

The cross-correlation is calculated with a time lag between frames of 10 ms to 50 ms and normalized by the cross-correlation of the average of the scintillation map on the CCD. The cross-correlation arrays provide the wind velocity of turbulence layers moving, at different velocity at different heights in the troposphere. It consists in a set of triplets (three peaks). The ratio between the position of the central peak of a triplet with respect to the center of the frame and the time lag ΔT give us the wind speed and the turbulence strength associated to that layer. The separation of the later peaks with respect to the central one give us the altitude of the turbulence layer with respect to the conjugated plane. The line joining the central peak of a each triplet with respect to the center of the cross-correlation frame gives us the wind direction.

We use an algorithm to automatically detect triplets that begins with finding all of the local maxima in the 2-d cross-correlation array (cf. [2,11,12]). Then, any of those peaks which are flanked by two equidistant peaks, within some tolerance, are considered a triplet. To avoid mismatching, the tolerance in x and y is kept at the intrinsic FWHM of the peaks, which is 4 pixels for ground-layer turbulence on our system.

Adjacent triplets that are closer than 4 pixels to each other are an elongated triplet and therefore discarded (similar to the visual inspection method[2]) because they are signature of wind fluctuations effects.

For example, with β Cygnus, the wide binary, we have kept 8,833 wind triplets out of the 5,412 cross-correlation measurements. For data reduction from the standard GS measurements there are 76,382 triplets in 16,657 measurements. The number of triplets in the case of wide binaries is strongly smaller because this technique can be applied only to the first hundreds of meters from the ground.

During our run we preferred to select a large time lag so to increase the dynamic and sensitivity near the ground. Indeed, as we will see later on, the most useful data retrieved from the standard GS in the wind speed configuration (or equivalently in the cross-correlation configuration) is the wind speed in the first 2 km. Analyses provided by the European Center for Medium Range Weather Forecast (ECMWF) provide a more efficient characterization of the wind speed at h $\geq$ 2 km.

3. STANDARD GENERALIZED SCIDAR - RESULTS

3.1 Discretized $C_n^2(h)$ profiles: Free Atmosphere

From the GS measurements in standard configuration, we calculated in the free atmosphere (h $\geq$ 1 km) the cumulative distribution of the integral (r_0 i.e. the Fried parameter) of all the C_N^2 profiles and we identify the three groups of profiles following the same procedure already employed on the same site[2] and above other sites.[2,13] The first group (*bad* discretized C_N^2 profile) corresponds to the profiles whose r_0 is within 20 % and 30 % of the total r_0 in the same vertical slab. Similarly we calculate the *typical* discretized C_N^2 profile whose r_0 falls between 45 % and 55 % of the total r_0 and the *good* discretized C_N^2 profile those profiles whose r_0 falls between 70 % and 80 % of the total r_0.

The profiles of each group are then discretized into bins (vertical slabs) with a Δh variable with respect to the height. We selected a vertical sampling of 500m just above 1 km, i.e. where the turbulence is more affected by orographic effects and therefore more sensitive to fluctuation in the spatial distribution and a lower vertical resolution in the high part of the atmosphere.

The bin boundaries we defined for Table 3 are in the first column. The next pair of columns are the mean height and turbulence integral in those bins for the *good* group, likewise for *typical* and *bad*. The mean turbulence integral J in each bin is the mean of the zeroth moment (Eqn.(3) in Appendix A). The mean height is computed as the first moment divided by the zeroth moment, simply a weighted average.

Table 3. Discretized C_N^2 profiles in the free-atmosphere (h $\geq$ 1 km)

	"good"		"typical"		"bad"	
bins	$h[m]$	$J[m^{1/3}]$	$h[m]$	$J[m^{1/3}]$	$h[m]$	$J[m^{1/3}]$
20000	16500	7.61e-15	16200	1.02e-14	16400	1.91e-14
14000	12900	5.10e-15	13000	9.65e-15	12900	1.57e-14
12000	10900	7.24e-15	10900	1.27e-14	10900	2.89e-14
10000	9050	8.52e-15	9070	1.72e-14	9080	3.22e-14
8000	6930	6.45e-15	7010	1.05e-14	6990	1.77e-14
6000	5020	9.50e-15	5030	1.23e-14	5080	2.10e-14
4000	3410	9.18e-15	3390	1.14e-14	3390	1.45e-14
3000	2490	1.97e-14	2470	3.39e-14	2450	4.02e-14
2000	1780	6.98e-15	1760	1.52e-14	1730	2.86e-14
1500	1240	5.28e-15	1240	1.50e-14	1270	2.86e-14
1000						

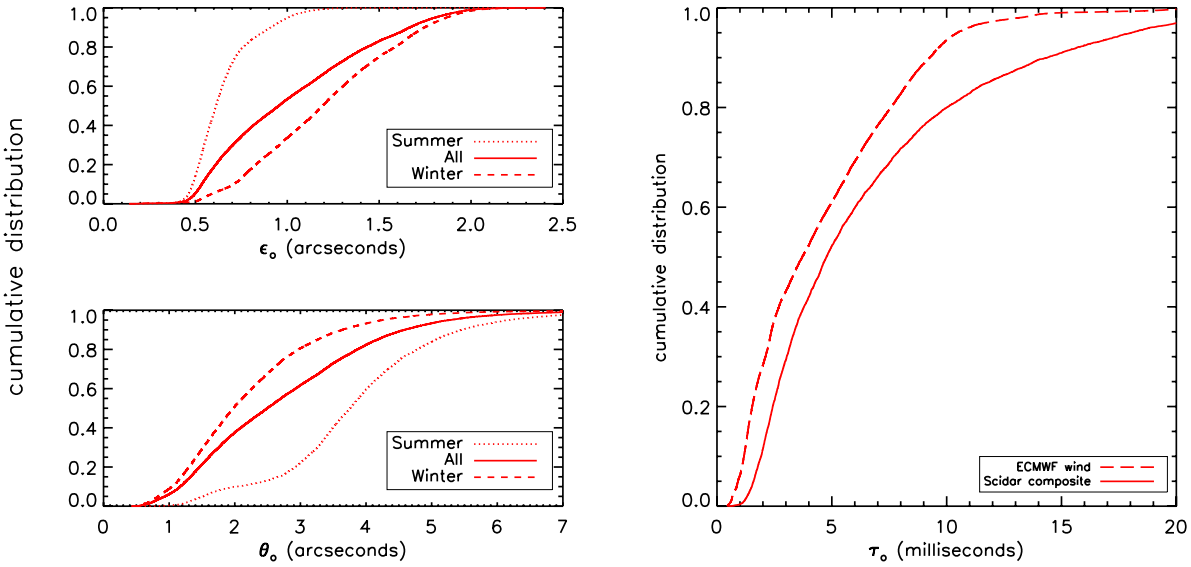

Figure 1. The full atmosphere cumulative distributions of the C_n^2 moments at Mt. Graham.

3.2 Integrated astroclimatic parameters

In Fig. 1-left side we show the cumulative distribution of the seeing (ε) and the isoplanatic angle (θ_0) above Mt. Graham associated to the sample of 43 nights (GS standard). The cumulative distribution of the same parameters measured in different seasons is also shown.

The median values of the integrated astroclimatic parameters are: the seeing ε_{tot}=0.95 arcsec, ε_{sum}= 0.61 arcsec, ε_{win}= 1.19 arcsec; the isoplanatic angle $\theta_{0,tot}$= 2.49 arcsec, $\theta_{0,sum}$= 3.76 arcsec, $\theta_{0,win}$= 1.98 arcsec. The median isoplanatic angle is now smaller (2.49 arcsec), down from 2.7 arcsec measured on the first 16 nights and published in Ref.[2]. However the typical value is still good with an interesting remarkably good median value θ_0= 3.76 arcsec in summer. In May 2005 and May 2007 we had, in both cases, 10-15 days of extremely good seeing and large isoplanatic angle.

Table 4. Classification the Scidar campaign measurements. GS standard: the vertical resolution is given by Eq.2 - Ref.[1], typically of the order of 1000 near the ground. GS - WB: vertical resolution of the order of 250 m near the ground. GS - HVR: vertical resolution of the order of 20-30 m.

Site	Instrument	Number of Nights	Number of hours
Mt. Graham	GS	43	163
Mt. Graham (*)	GS	16	42
Dome C	MASS	22	30
Cerro Pachon	MASS	21	160
Cerro Tololo	MASS	152	760

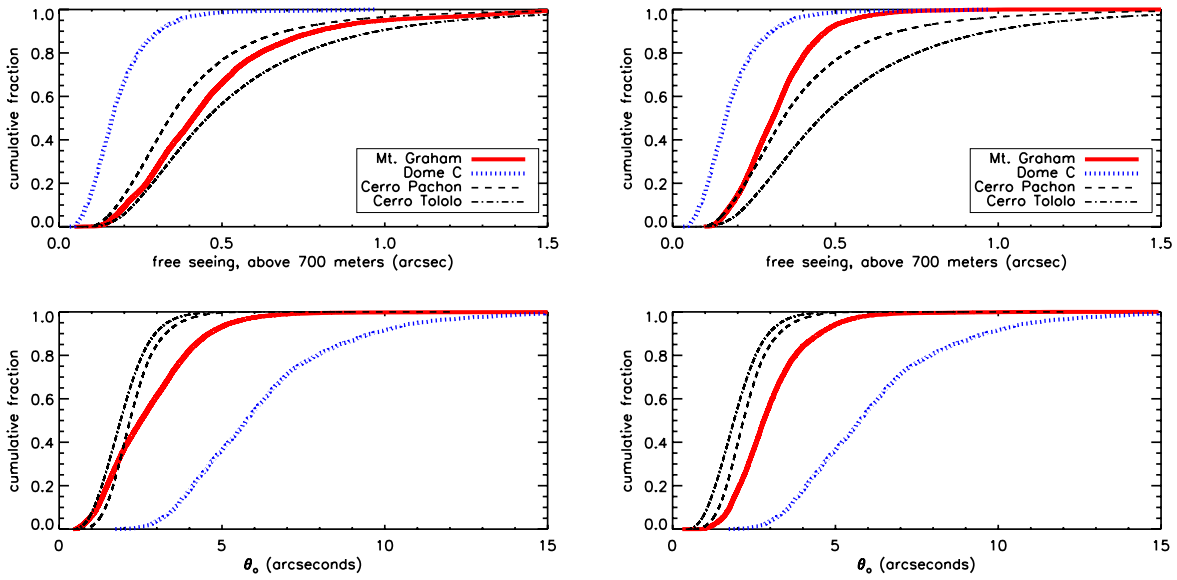

Figure 2. The cumulative distribution of free seeing (integrated only above 700 meters) compared with MASS measurements at other sites (upper plot) as well as isoplanatic angle (lower plot).

In Fig. 1-right side is the best estimated distribution (solid line) of coherence time Eqn.(7). In bold line is shown the τ_0 calculated using a composite wind speed. Below 2 km we take the wind speed retrieved from the GS and, above 2 km, we take the wind speed from the European Center for Medium Range Weather Forecast (ECMWF) analyses extracted in the nearest grid point to the Mt. Graham (32.75^{o}N and 110.00^{o}W, 20 km northwest of the summit). It has been already proved[2] that this method is the most efficient way to calculate τ_0. In dashed line we show the τ_0 calculated with the wind speed from the ECMWF analyses [‡] extended from the ground up to the top of the atmosphere.[14] This method aims to calculate τ_0 without the support of a GS but it introduces necessarily a bias (worse τ_0) above a site located on the summit of a mountain because in the integral of the C_N^2 and the $v(h)$ we take into account turbulence and wind speed below the altitude of the site. We show this second option to warn people from using a solution that can appear simpler and faster but it is affected by a bias. To maximize our statistic we used, in both cases (solid and dashed line), the $C_n^2(h)$ extracted from the auto-correlation frames. We are indeed interested in the statistic of the τ_0 and the wind speed fluctuates on a

[‡]The ECMWF wind profiles are computed from a general circulation model based on a set of spatio-temporal interpolations of measurements provided by meteorological stations distributed on the surface of the whole world, and by satellites and instruments carried aboard aircraft. Analyses are extracted from the MARS (Meteorological Archival and Retrieval System) catalog.

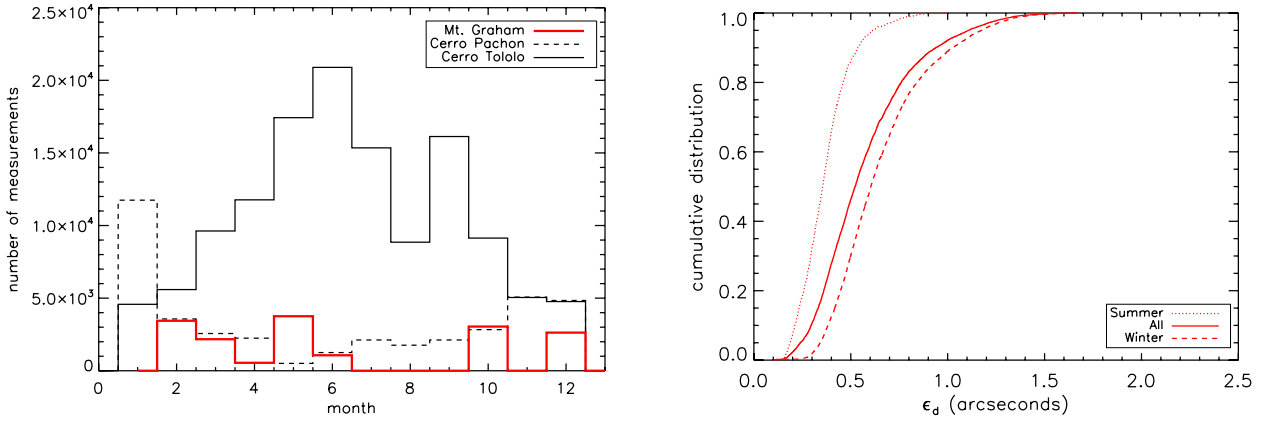

Figure 3. **Left**: Histogram of the seasonal distribution of measurements done above Mt.Graham, Cerro Pachon and Cerro Tololo and used to calculate Fig.2. **Right**: The cumulative distribution of the dome seeing from the GS standard selection - Table 1

larger spatial scale than that typical of the C_N^2 . This means that the wind speed change on longer time scales. The $v(h)$ extracted from the ECMWF analyses is interpolated as in [2] to match the height grid of $C_n^2(h)$. The median wavefront coherence time obtained with the composite wind speed profile is $\tau_{0,tot}$= 4.02 msec. We highlight that all results shown in this section have been obtained with the C_N^2 profiles extended on the whole troposphere i.e. from the ground up to 20 km including the dome seeing.

3.3 Site comparison

In this section we present a comparison of a few integrated astroclimatic parameters measured above Mt. Graham and three other sites: Dome C (Antarctica), Cerro Pachon (Chile) and Cerro Tololo (Chile). Table 4 reports the instruments used at each site to measure the optical turbulence and the relative statistical sample (number of nights and total hours of observations) that we considered in our estimates.

Due to the fact that the MASS do not sense the first hundred of meters, to perform a fair comparison between sites using different instruments GS and MASS, we limited the comparison to h $\geq$ 700 m and we focused our attention on two parameters: **(1)** the seeing above 700 m **(2)** the isoplanatic angle θ_0. We highlight that the first hundreds of meter of turbulence do not provide any contribution to θ_0 because of the weighting function $h^{5/3}$. In Appendix A are reported the analytical expression of the moments (seeing and isoplanatic angle).

The MASS data from Dome C refer to Ref.[15], the Cerro Pachon and Tololo data refer to Web Site[§] and they have been downloaded on 2006-12-29.

The top panel of Fig. 2-left shows the cumulative distribution of the seeing above 700 meters calculated above the four sites. The bottom panel shows the isoplanatic angle. On Fig. 2-right we have the same cumulative distribution but related to the first 16 nights. The statistic on a limited number of night is reported to show that these comparisons are pretty sensitive to the richness of the sample used. We observe at Mt. Graham median values of seeing and isoplanatic angles comparable to those measured above other sites among the best in the world.

Dome C has, in this plot, remarkably good seeing and isoplanatic angle that seem to be substantially better than those measured above the mid-latitude ones. We highlight however that more recent measurements[16] indicated that the difference between mid-latitude sites and Dome C is more modest.

A further element that should be taken into account in this kind of comparison is the seasonal-bias. It is indeed known that there are periods of potentially better and worse seeing. Normally (apart local effects) the good period corresponds, for sites in the North Hemisphere, to the spring/summer time and the bad period

[§] $http://139.229.11.21/massindex.php$

to the winter time. In the South Hemisphere the situation is inverted. Fig.3-left shows the histogram of the seasonal distribution of measurements done above three out the four sites we analyzed in Fig.2. Mt. Graham is located in the North Hemisphere while Cerro Pachon and Cerro Tololo in the South one. It can be seen that, at Mt.Graham and Cerro Tololo (the effect is particularly evident above this site), there are more measurements associated to their worst period while at Cerro Pachon there are more measurements associated to the best one. This means that the estimates given in Fig.2, in a more homogeneous statistic sample, might provide median values slightly shifted towards better seeing values at Cerro Tololo and Mt.Graham and towards worse seeing values at Cerro Pachon.

4. THE GROUND-LAYER

4.1 Dome seeing

The statistic that we have discussed for the seeing relates to the whole turbulence contribution included the dome seeing. To quantify the contribution provided only by the atmosphere we have to subtract from the total seeing the dome contribution to be calculated with the method described in Ref.[2, 9]. The method consists in discriminating the triplets located at the ground with a velocity equal to zero and those with a velocity different from zero. The velocity resolution of our system is 0.8 to 0.2 m/s per pixel for time lags from 1 to 4 frames (10 to 40 ms). Triplets located at the ground (H= $0\pm\Delta H$) with ΔH given by Eqn.2 (Ref.[1]) and within the unresolved velocity are called the 'zero velocity' component. In order to provide an unambiguous dome seeing measurement, a cross-correlation measurement must also have at least one triplet in the surface-layer and a resolved non-zero velocity.[9]

Fig. 3-right shows the cumulative distribution of the dome seeing (ε_d). The median value is ε_d= 0.52 arcsec. For the first time we observe an interesting seasonal trend in the dome contribution and such a feature will be certainly carefully investigated in the future. **Knowing that the median seeing in the whole atmosphere (included the dome seeing) is 0.95 arcsec (Sec.3.2) and that ε_d= 0.52 arcsec, we deduce that the median seeing related to the whole atmosphere without the dome contribution for the richest statistic we collected so far (43 nights) is therefore ε_{tot}= 0.72 arcsec**.

4.2 Discretized $C_n^2(h)$ profiles: Boundary Layer

In Table 5 we report the same discretization done in Table 3 for the free atmosphere but using the GS - WB data-set (see Table 1) in the first kilometer. This data set of C_N^2 profiles is characterized by an intrinsic vertical resolution of the order of 200-250 m. This value (200-250 m) corresponds also to the vertical resolution required to optimize the LGS/GLAO system of LBT (D = 8 m, pitch size Δ = 0.5 m and a field of view θ = 4 arcmin) . The required vertical resolution is indeed, established by the value of the gray-zone. The gray-zone (Δ/θ), i.e. the heigth above which the turbulence is partially corrected by a GLAO system, is $\sim$ 250 m for the optical configuration of the LBT system.

However, to obtain an optical turbulence vertical distribution at such a vertical resolution with the best statistic reliability we have to multiply each element of each column in Table 5 for the factor $f_{gl}=(\varepsilon_o/\varepsilon'_o)^{5/3}$ (see Table 6) where ε_o is the total seeing in the first kilometer for the 43 nights GS-Standard sample and ε'_o is the same for the 23 nights of the GS-WB sample. These two statistical samples are not homogeneus. The correction with the factor f_{gl} is done to preserve the total turbulent energy that has been monitored by the GS-Standard near the ground on 43 nights (ε_o). The latter is the richest sample we have; it is therefore the more representative from the point of view of the total energy in the first kilometer. This operation corresponds to a redistribution of the turbulence in the first kilometer following the typical decay law given by the GS-WB data set. Joining the Table 5 opportunely corrected by f_{gl} and Table 3 one can obtain nine different combinations of *good, typical,* and *bad* distributions in the whole atmosphere (ground layer and free atmosphere) to set-up the parameter space for simulations for the LGS/GLAO system of LBT. Table 7 reports the composite seeing table obtained with the 9 possible combinations. We highlight that the median dome seeing (ε_d) has been estimated equal to = 0.52 arcsec. This means that, to retrieve the seeing purely given by the atmosphere from Table 6 and Table 7 one should opportunely subtract this offset.

Table 5. Discretized C_N^2 profiles in the boundary layer (h $\leq$ 1 km)

	"good"		"typical"		"bad"	
bins	$h[m]$	$J[m^{1/3}]$	$h[m]$	$J[m^{1/3}]$	$h[m]$	$J[m^{1/3}]$
1000.0	949	2.02e-15	947	5.47e-15	947	7.34e-15
900.0	849	1.50e-15	851	3.24e-15	853	3.38e-15
800.0	750	1.60e-15	742	4.26e-15	745	6.23e-15
700.0	647	2.39e-15	650	7.16e-15	655	1.18e-14
600.0	557	1.91e-15	560	5.32e-15	563	7.59e-15
500.0	452	1.40e-15	453	5.48e-15	456	1.02e-14
400.0	343	4.92e-15	354	2.52e-14	353	4.60e-14
300.0	251	6.11e-15	272	8.17e-15	258	1.28e-14
200.0	136	1.45e-14	118	2.65e-14	120	4.50e-14
100.0	5	9.68e-14	2	2.22e-13	2	3.34e-13
-100						

4.3 GS - High Vertical Resolution

The vertical distribution at high resolution (20-30 m) is obtained with the method presented in Ref.[1]. The GS-HVR data-set is obtained taking the integral of the C_N^2 profiles retrieved from the auto-correlation array and then redistributing this energy vertically using the detectable triplets in the cross-correlation array. Fig.4 shows the mean of the C_N^2 profiles at high vertical resolution of 8 nights (asterisks) extracted from the sample GS-HVR (Table 1). To retrieve the typical scale height (B) of the exponential decay we fitted the measurements done below 125 m with an exponential law (Eqn.2, dashed line in Fig.4):

$$y = A \cdot e^{(-h/B)} \tag{2}$$

The fit is obtained with A=$1.3{\cdot}10^{-14}$ and B=22 m. We observe that the optical turbulence vertical dis-

Table 6. Seeing in the boundary layer

Ground Layer Seeing	good	typical	bad
A. GS standard (ε_o)	0.55	0.81	1.16
B. GS - WB (ε'_o)	0.38	0.63	0.81
f_{gl}	1.9	1.5	1.8

Table 7. Composite Seeing (arcsec)

Composite Seeing	GL: *good*	GL: *typ*	GL: *bad*
FA: *good*	0.66	0.90	1.23
FA: *typ*	0.73	0.95	1.27
FA: *bad*	0.83	1.04	1.35

tribution obtained with the GS-HVR data set is much more sharp that what normally reconstructed by the GS-standard measurements. The turbulence decreases of ~ 2 order of magnitude in the first 100 m. We highlight that, in this vertical distribution, the dome seeing is included therefore a further contribution should be subtracted to quantify the effective turbulence near the ground typical of the site itself. This should be done with the *'5/3 law'* usually employed to add/subtract partial seeing components.

Table 8 shows the percentage of the turbulence located below 30 m (height of the LBT primary mirror from the ground) with respect to the turbulence in the whole 20 km for all the 8 nights studied in this paper. In this last calculation the dome seeing has been subtracted. We observe that, the turbulence distribution scales in a pretty sharp way and a consistent percentage of turbulence develops in the first 30 m from the ground. A sharp vertical distribution is a promising scenario for GLAO-AO correction system. The analysis of the whole GS-HVR data-set collected so far is on-going.

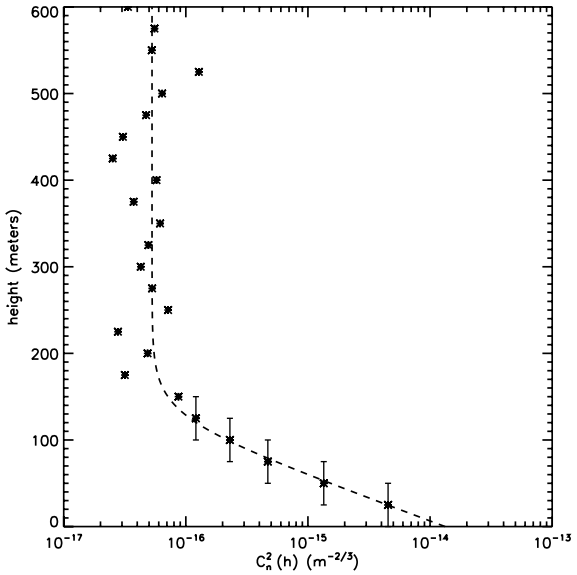

Figure 4. Asterisks: Mean C_N^2 profile ($\Delta h \sim$20-30 m) calculated with the method described in Ref.[1] with the sample C. (Table 1). Dashed line: analytical fit.

Table 8. Percentage (%) of turbulence developed below 30 m (LBT primary mirrror height from the ground) in 8 different nights.

Night	1.	2.	3.	4.	5.	6.	7.	8.
(%)	69	60	43	62	25	41	58	33

5. CONCLUSIONS

In this paper we present the status report of an on-going study aiming to characterize the optical turbulence at Mt. Graham. We present a general overview of the statistics (43 nights) of all the main integrated astroclimatic parameters and their seasonal trends. With a median seeing ε= 0.95 arcsec (ε= 0.72 arcsec without dome contribution), isoplanatic angle θ_0= 2.49 arcsec and a wavefront coherence time τ_0=4.02 msec, Mt. Graham confirms its good quality in terms of turbulence characteristics typical of the best astronomical sites in the world. The ground layer is characterized for the first time with such a high statistical reliability with a resolution of 200-250 m (23 nights) and 20-30 m (8 nights) and a composite distribution of the turbulence on the whole 20 km

is calculated to be used as input of AO simulations representing a suitable parameters space for this astronomical site. The main conclusions we achieved are:

- The turbulence exponentially decays above Mt. Graham with a much sharper profile than what supposed so far. It is the first time that such a trend has been put in evidence above a mid-latitude site.
- The percentage of turbulence developed in the first 30 m above the ground (below the primary mirror of the LBT) is mostly larger than 30%. This interesting last result needs certainly to be confirmed with a richer statistic. However, this trend, joint with the favorable large θ_0 in the spring/summer time are conditions particularly favorable for astronomical observations assisted by a LGS/GLAO system.
- For the first time, we observed a seasonal trend of the dome seeing. This is certainly a topic that is worth of a more careful investigation in the future.

APPENDIX A. MOMENTS FROM $C_n^2(h)$

A useful metric for distribution functions is its moment. There are two moments that are commonly used in astroclimatology because of their connection to observable quantities, either at the focal plane or in an adaptive optics system. The m^{th} moment of the $C_n^2(h)$ distribution function is

$$\mu_m = \int dh\ C_n^2(h)\ h_i^m. \tag{3}$$

The m^{th} moment of the product of the distributions of $C_n^2(h)$ and wind speed, $v(h)$, is

$$\upsilon_m = \int dh\ C_n^2(h)\ v^m(h). \tag{4}$$

Since we measure a discretized $C_n^2(h)$ we approximate each of the above integrals as a sum over the available ordered pairs of numbers $v_j(h_j)$, and the ordered pairs of $C_{ni}^2(h_i)$. For $C_{ni}^2(h_i)$ from Scidar we start the sum from -1 km since the computation of $C_{ni}^2(h_i)$ from the auto-correlation profile leaves a small but non-negligible residue at negative heights.

The above moments are related to the following quantities: seeing

$$\epsilon_o = 0.98\ \lambda^{-1/5}\left[0.4232(2\pi)^2\mu_o\right]^{3/5}, \tag{5}$$

isoplanatic angle

$$\theta_o = \left[2.91\left(\frac{2\pi}{\lambda}\right)^2\mu_{5/3}\right]^{-3/5}, \tag{6}$$

and the coherence time

$$\tau_o = \left[2.91\left(\frac{2\pi}{\lambda}\right)^2\upsilon_{5/3}\right]^{-3/5}. \tag{7}$$

These quantities are named for their relationship to properties of the wavefront or the image of a star.[17] We use the wavelength $\lambda = 0.5\mu m$.

ACKNOWLEDGMENTS

This work is funded by the Marie Curie Excellence Grant (FOROT) MEXT-CT-2005-023878, FP6 Program. We thanks the VATT and LBT staff for the support we had during the recent Scidar observing runs. We thank John Storey's team for providing the Dome C MASS data and Mark Chun for providing the Mauna Kea MASS data related to the paper Tokovinin et al. (2005).

REFERENCES

1. Egner, S. E. and Masciadri, E., "A G-SCIDAR for Ground-Layer Turbulence Measurements at High Vertical Resolution," *PASP* **119**, 1441–1448 (Dec. 2007).
2. Egner, S. E., Masciadri, E., and McKenna, D., "Generalized SCIDAR Measurements at Mount Graham," *PASP* **119**, 669–686 (June 2007).
3. Masciadri, E., Avila, R., and Sánchez, L. J., "Statistic Reliability of the Meso-Nh Atmospherical Model for 3D C[N]2 simulations," *Revista Mexicana de Astronomia y Astrofisica* **40**, 3–14 (Apr. 2004).
4. Masciadri, E., "Optical turbulence forecast: toward a new era of ground-based astronomy," in [*Ground-based and Airborne Telescopes. Edited by Stepp, Larry M.. Proceedings of the SPIE, Volume 6267, pp. 62671C (2006).*], *Presented at the Society of Photo-Optical Instrumentation Engineers (SPIE) Conference* **6267** (July 2006).
5. Rabien, S. e. a., "The Laser Guide Star Program for the LBT," *SPIE* (2008).
6. McKenna, D. L., Avila, R., Hill, J. M., Hippler, S., Salinari, P., Stanton, P. C., and Weiss, R., "LBT facility SCIDAR: recent results," in [*Adaptive Optical System Technologies II. Edited by Wizinowich, Peter L.; Bonaccini, Domenico. Proceedings of the SPIE, Volume 4839, pp. 825-836 (2003).*], Wizinowich, P. L. and Bonaccini, D., eds., *Presented at the Society of Photo-Optical Instrumentation Engineers (SPIE) Conference* **4839**, 825–836 (Feb. 2003).
7. Rocca, A., Roddier, F., and Vernin, J., "Detection of atmospheric turbulent layers by spatiotemporal and spatioangular correlation measurements of stellar-light scintillation.," *Journal of the Optical Society of America (1917-1983)* **64**, 1000–1004 (1974).
8. Vernin, J. and Azouit, M., "Image processing adapted to the atmospheric speckle. II. Remote sounding of turbulence by means of multidimensional analysis.," *Journal d'Optique* **14**, 131–142 (1983).
9. Avila, R., Vernin, J., and Sánchez, L. J., "Atmospheric turbulence and wind profiles monitoring with generalized scidar," *A&A* **369**, 364–372 (Apr. 2001).
10. Mason, B. D., Wycoff, G. L., Hartkopf, W. I., Douglass, G. G., and Worley, C. E., "The 2001 US Naval Observatory Double Star CD-ROM. I. The Washington Double Star Catalog," *AJ* **122**, 3466–3471 (Dec. 2001).
11. Avila, R., Carrasco, E., Ibañez, F., Vernin, J., Prieur, J.-L., and Cruz, D. X., "Generalized SCIDAR Measurements at San Pedro Mártir. II. Wind Profile Statistics," *PASP* **118**, 503–515 (Mar. 2006).
12. Prieur, J.-L., Avila, R., Daigne, G., and Vernin, J., "Automatic Determination of Wind Profiles with Generalized SCIDAR," *PASP* **116**, 778–789 (Aug. 2004).
13. Tokovinin, A. and Travouillon, T., "Model of optical turbulence profile at Cerro Pachón," *MNRAS* **365**, 1235–1242 (Feb. 2006).
14. Geissler, K. and Masciadri, E., "Meteorological Parameter Analysis above Dome C Using Data from the European Centre for Medium-Range Weather Forecasts," *PASP* **118**, 1048–1065 (July 2006).
15. Lawrence, J. S., Ashley, M. C. B., Tokovinin, A., and Travouillon, T., "Exceptional astronomical seeing conditions above Dome C in Antarctica," *Nature* **431**, 278–281 (Sept. 2004).
16. Trinquet, H., Agabi, A., Vernin, J., Azouit, M., Aristidi, E., and Fossat, E., "Nighttime Optical Turbulence Vertical Structure above Dome C in Antarctica," *PASP* **120**, 203–211 (Feb. 2008).
17. Roddier, F., [*Adaptive optics in astronomy*], Adaptive Optics in Astronomy (1999).